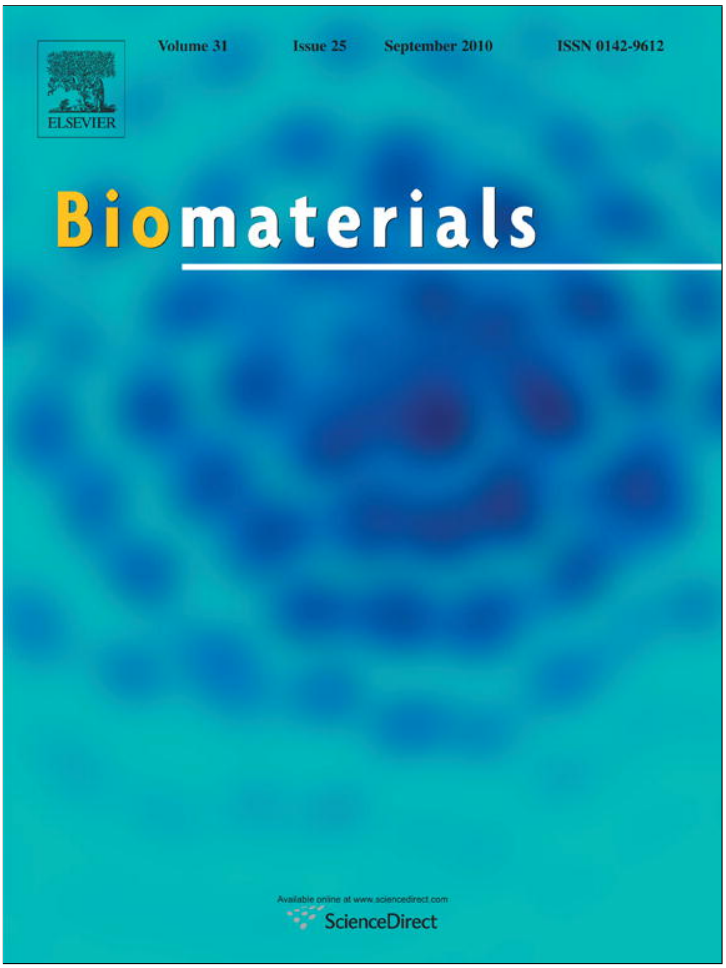

Biomaterials 31 (2010) 6511–6518

Contents lists available at ScienceDirect

Biomaterials

journal homepage: www.elsevier.com/locate/biomaterials

The control of stem cell morphology and differentiation by hydrogel surface wrinkles

Murat Guvendiren, Jason A. Burdick*

Department of Bioengineering, University of Pennsylvania, 210 S 33rd Street, Philadelphia, PA 19104, USA

ARTICLE INFO

Article history:
Received 15 April 2010
Accepted 18 May 2010
Available online 11 June 2010

Keywords:
Hydrogel
Surface wrinkles
Stem cells
Morphology
Differentiation

ABSTRACT

In this study, we investigated human mesenchymal stem cell (hMSC) interactions with uniform hydrogels and hydrogels with lamellar or hexagonal surface wrinkles to elucidate our ability to control hMSC morphology and differentiation. Wrinkled hydrogels were prepared from photocurable poly(2-hydroxyethyl methacrylate) (PHEMA) precursor solutions containing ethylene glycol dimethacrylate as a crosslinker, using depth-wise gradients in crosslinking and subsequent buckling with swelling to generate wrinkles. A replica molding process was used to fabricate a series of gels with uniform mechanics, but altered surface wrinkle size and shape. We found that hMSCs attached to lamellar wrinkles spread by taking the shape of the pattern, exhibit high aspect ratios, and differentiate into an osteogenic lineage. In contrast, cells that attached inside the hexagonal patterns remain rounded with low spreading and differentiate into an adipogenic lineage. This work aids in the development of material-based cell culture and scaffold systems to direct stem cell differentiation.

1. Introduction

Human mesenchymal stem cells (hMSCs) are marrow-derived heterogeneous cells that are able to proliferate and differentiate into a variety of cell types, such as osteoblasts (bone), adipocytes (fat), and chondrocytes (cartilage) [1,2]. Due to their migratory and space filling ability, potential as a clinically translatable autologous cell source, and multi-lineage potential, the use of hMSCs has become increasingly important as a component in approaches for wound repair and tissue regeneration [3,4]. Therefore, it is crucial to understand mechanisms for controlling hMSC differentiation to generate novel regenerative stem cell-based therapies.

Stem cells are responsive to both intrinsic and extrinsic cues, which include soluble factors [2], chemical and physical signals [5–9], mechanical factors [10,11] (such as matrix elasticity and tension) and the general microenvironment [12–14]. In response to complex spatial and temporal combinations of these cues, such as in the natural extracellular matrix environment, cells undergo morphological changes and lineage specification. For example, Engler et al. showed that matrix elasticity can specify stem cell lineage toward neurons, myoblasts and osteoblasts [11]. While these cues may cause morphological changes along the path to differentiation, it was also shown that cell shape alone could regulate stem cell differentiation [15–17]. For instance, by generating fibronectin coated islands with various sizes on flat surfaces, McBeath et al. showed the switch in hMSC commitment from adipogenic to osteogenic phenotypes with increasing island size from 1024 to 10,000 μm^2, which was reported to regulate cellular RhoA activity [18]. In addition, Ruiz and Chen showed that the overall geometry of the patterns is important to regulate proliferation, spreading and differentiation [19]. They concluded that the relative location of the individual cells within a pattern determines the localized cytoskeletal tension, triggering differentiation such that high tension leads to greater spreading and osteogenesis, whereas low tension leads to rounded cells and adipogenesis. Finally, Kilian et al. recently showed the critical role of geometric shape in regulating mechanochemical signals and paracrine/autocrine factors to direct MSC differentiation [20].

In this study, we investigated a technique to control stem cell morphology and differentiation: namely micro-scale hydrogel surface wrinkling. Micro- and nano-structured patterns on elastomeric and hard materials are able to control cell orientation, elongation, growth and migration for various cell types, mainly due to contact guidance and the extent of focal adhesions, determined by the feature dimensions [21–24]. First, we investigated the effects of wrinkle morphology and size on stem cell shape, with particular interest on the wrinkle conditions for rounded cells with low spreading, and for elongated cells with high aspect ratios. Then, we investigated the effects of this controlled cell shape and

* Corresponding author. Tel.: +1 215 898 8537; fax: +1 215 573 2071.
E-mail address: burdick2@seas.upenn.edu (J.A. Burdick).

0142-9612/$ – see front matter © 2010 Elsevier Ltd. All rights reserved.
doi:10.1016/j.biomaterials.2010.05.037

spreading on hMSC differentiation towards osteogenic and adipogenic phenotypes.

2. Materials and methods

2.1. Fabrication of hydrogels with surface wrinkling

Surface patterns formed spontaneously on PHEMA hydrogels with depth-wise crosslinking gradients when immersed in water, and remained stable in the dry state. The details of the pattern formation, ordering and characterization can be found elsewhere [25,26]. In this study, we used previously fabricated gradient-PHEMA gels (i.e., PHEMA masters) with lamellar and hexagonal surface patterns, and replicated these patterns on PHEMA gels with uniform structural and mechanical properties using a replica molding technique. PHEMA prepolymer was prepared by UV exposure (UVP Black Ray, 8 mW cm^{-2}) of 2-hydroxyethyl methacrylate (HEMA, 2.5 mL, 98%, Alfa Aesar) as monomer and Darocur 1173 (3 wt%, 75 μL, Ciba Specialty Chemicals) as photoinitiator for 1 min. Additional Darocur 1173 (50 μL) and the crosslinker, ethylene glycol dimethacrylate (EGDMA, 25 μL, Polysciences), was added to the prepolymer to form PHEMA molding precursor. A PDMS mold was fabricated by casting the PDMS precursor mixed with the curing agent (Sylgard 184® Silicone Elastomer Kit, Dow Corning) in a 10 to 1 weight ratio onto the PHEMA master, followed by thermal curing at 65 °C for 4 h. The PDMS mold was then carefully peeled off from the PHEMA master. To fabricate the PHEMA replica, PHEMA molding precursor was cast on a methacrylated glass slide [25] and the PDMS mold was pressed over it. The PDMS mold was gently peeled off after UV exposure (Omnicure S1000 UV Spot Cure System, Exfo Life Sciences Division) for 25 min (~10 mW cm^{-2}, 365 nm). The crosslinked PHEMA film (PHEMA replica) attached to the glass slide was incubated at 140 °C for 2 h in order to further crosslink the reactive components in the gel.

2.2. Preparation of hydrogel substrates for cell studies

PHEMA replicas attached to the glass slides were placed in a 24-well plate, swelled in PBS (refreshed several times) and in 70% ethanol (in PBS) for 1 day each, and sterilized under a germicidal UV lamp for 2 h. Hydrogels were then incubated in fibronectin from bovine plasma (20 μg mL^{-1}, Sigma) in DPBS (Dulbecco's phosphate buffered saline 1×, 1 mL per well) at 37 °C overnight. After the solution was aspirated, wells were rinsed with DPBS three times, and hydrogel films were maintained in 0.5 mL of growth medium in each well at 37 °C for 1 h prior to cell seeding.

2.3. Imaging wrinkle morphology and fibronectin adsorption

In order to characterize the distribution of fibronectin on the hydrogel surfaces, fibronectin was conjugated with FITC by using a FluoroTag™ FITC conjugation kit (FITC1-1KT, Sigma). Both bright field and fluorescent microscopy imaging was performed either on Olympus BX51 microscope (B&B Microscopes Limited) and Zeiss Axiovert 200 inverted microscope (Hitech Instruments, Inc.). Confocal microscopy imaging was performed on a Nikon TE300 inverted microscope fitted with a Bio-Rad Radiance 2000 MP3 system (Bio-Rad Laboratories, Inc.). Images were observed through a 10× and/or 20× objective, and recorded with Lasersharp 2000 software (Bio-Rad Laboratories, Inc.). A fluorescent dye, methacryloxyethyl thiocarbonyl rhodamine B (PolyFluor™ 570, Polysciences), was added to the precursor to obtain contrast (gel appears red under fluorescent light). Depth profiles were obtained by collecting xz-scans with 1 μm step size.

2.4. Cell culture and reagents

Human mesenchymal stem cells (hMSCs, Lonza Corp.) were expanded in growth medium (α-MEM, 10% FBS, 1% L-glutamine and 1% penicillin streptomycin). HMSCs (passage 3) were exposed to 10 μg mL^{-1} mitomycin C (Sigma) in serum-free growth medium for 2 h, washed with growth medium several times, and incubated in growth medium for at least 1 h prior to seeding. For spreading and morphology studies, cells were seeded on flat and surface patterned PHEMA hydrogels (3 gels per condition) in a 24-well plate and incubated for 24 h in the growth medium (1 mL of media per well). For differentiation studies, after 24 h of incubation in growth medium, cells were maintained in 1:1 adipogenic induction (Lonza Corporation): osteogenic (R&D Systems Inc.) media (mixed media) for 14 days. Media was refreshed every 3 days.

2.5. Cell staining

Cells were washed and fixed in 4% formalin for 10 min. For morphology studies, after triton extracting the soluble component and blocking the non-specific binding sites (with 3% BSA and 0.1% Tween-20 in PBS), the samples were stained for actin with FITC-phalloidin (Sigma) and for nuclei with DAPI (Invitrogen). For differentiation studies, fixed cells were stained for alkaline phosphatase with Fast Blue RR/naphthol solution (Sigma), lipid droplets using 3 mg mL^{-1} oil red O (Sigma) in 60% isopropanol, and nuclei with DAPI. Cells were also fixed and immunostained on other samples for fatty acid binding protein 4 (FABP4) and osteocalcin. After fixing and triton extracting the soluble components, samples were blocked for 1 h with

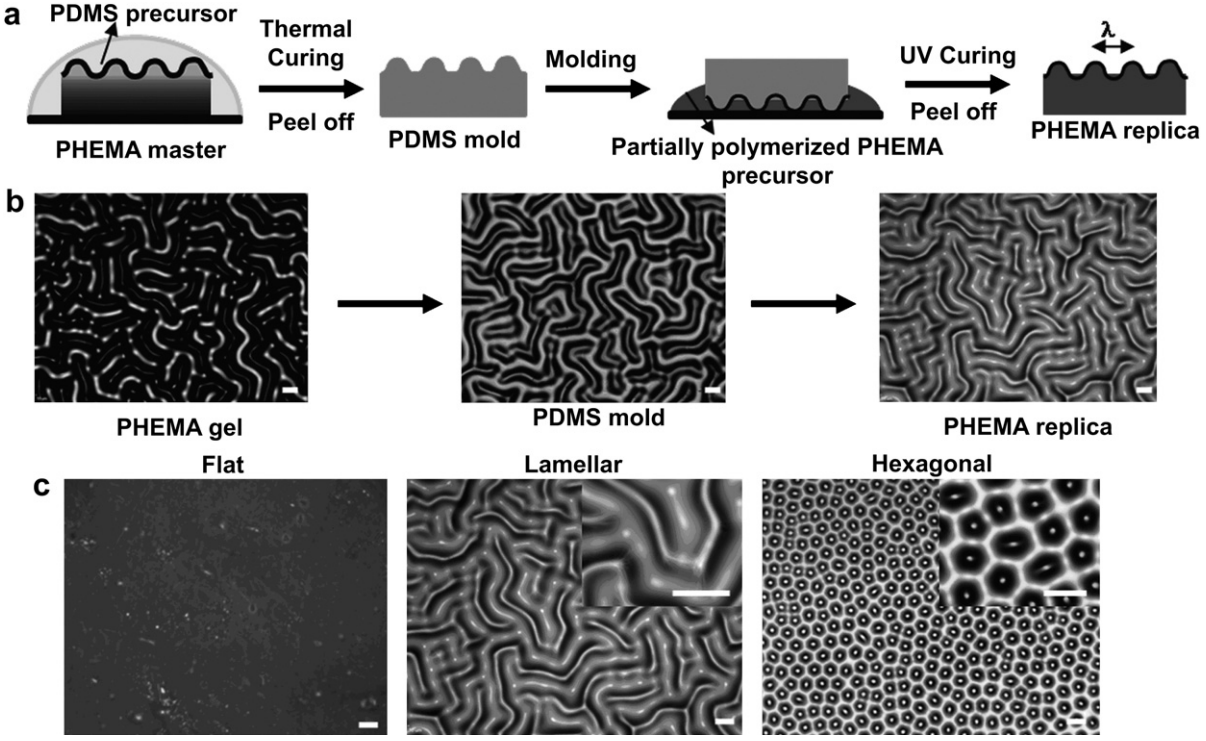

Fig. 1. (a) Schematic of the patterned-hydrogel fabrication process. (b) Optical microscopy images of the original, gradient-PHEMA gel with swelling surface patterns, PDMS mold and PHEMA replica. (c) PHEMA gels containing 1 wt% EGDMA with uniform mechanical properties (~150 kPa), but different surface topography: flat, lamellar and hexagonal. Scale bars are 50 μm.

33% goat serum. Samples were then incubated in anti-human FABP4 (R&D Systems Inc.) and osteocalcin (R&D Systems Inc.) antibodies overnight, followed by incubation in Alexa Fluor^R 488 goat anti-mouse IgG (H + L) (Invitrogen, Molecular Probes) and Alexa Fluor^R 350 donkey anti-goat IgG (Invitrogen, Molecular Probes) secondary antibodies for 1 h, followed by extensive washing.

For cellular aspect ratio measurements, at least 10 images (combination of bright field and fluorescent microscopy images at 10× magnification) were taken from each hydrogel surface (3 gels for each condition). Maximum orthogonal length, width and area of each cell were measured using NIH ImageJ (1.41n), and the aspect ratio was calculated as the longer length divided by the shorter length.

3. Results and discussion

We recently reported the formation of a wide range of surface wrinkling patterns: random worm-like structures, peanut shape, lamellar and a highly ordered hexagonal pattern, in swollen poly(2-hydroxyethyl methacrylate) (PHEMA) gradient-hydrogel films confined onto a flat substrate [25,26]. Gradient hydrogels were fabricated by manipulating O_2 diffusion during the UV curing process, which created a modulus gradient with depth. Wrinkle morphology and size were controlled by the crosslinker concentration and initial film thickness, respectively. In addition, the resulting surface wrinkles were kinetically trapped during drying because of the glassy nature of PHEMA, leading to stable patterns in both wet and dry states. Although we obtained reproducible pattern structures and sizes, the structural and mechanical properties of the hydrogel films differ significantly for each condition [25]. Therefore, in order to decouple PHEMA properties from the wrinkle morphology and size, we produced replica gels from gradient-PHEMA masters in two-steps (Fig. 1a and b). First, a PDMS mold was generated from the master. Next a PHEMA replica was created by pressing the PDMS mold on a partially polymerized PHEMA precursor cast on a methacrylated glass slide and exposing it to UV light (Fig. 1b). Importantly, this technique is applicable to a variety of photocrosslinkable materials. For instance, for methacrylated hyaluronic acid gels [27,28], wrinkle geometry remained stable for gels with equilibrium Young's modulus >100 kPa (results not shown).

To investigate the effects of pattern geometry and size on stem cell morphology and spreading, we focused on lamellar and hexagonal patterns with $\lambda = 50$ or 100 μm (amplitude ~ 20 μm) for each condition (Figs. 1c and 2, also see Fig. S1 in the Supporting Information). Replica gels with surface patterns or flat gels were photocured from a PHEMA precursor solution containing 1 wt% EGDMA (crosslinker) and exhibited swollen Young's moduli of ~150 kPa, regardless of pattern type or size [25]. After sterilization, hydrogels were incubated in a fibronectin solution to enhance cell adhesion, and fibronectin was found to diffuse uniformly into the

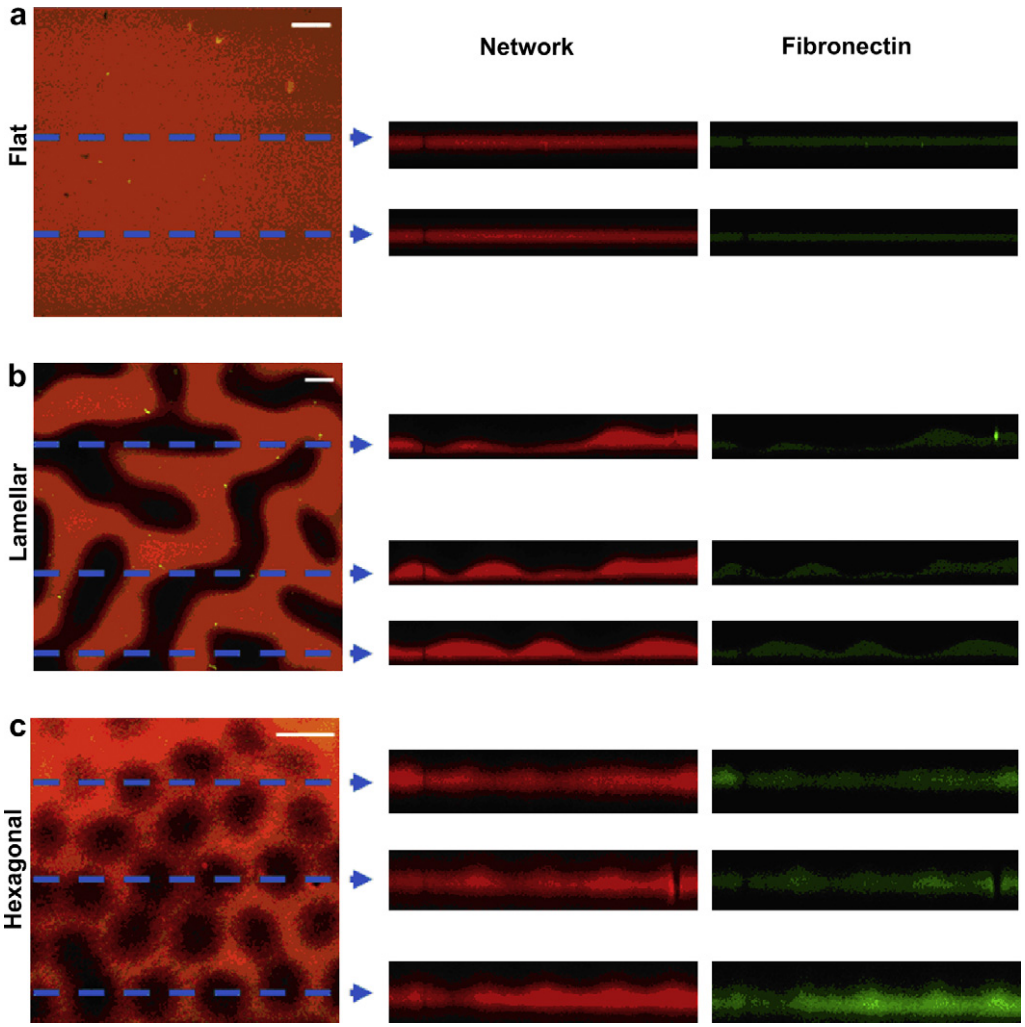

Fig. 2. Confocal fluorescent microscopy images (xy- and xz-scans) of PHEMA hydrogels: without (flat) and with either lamellar or hexagonal surface patterns stained for either the network structure (red) or for fibronectin localization (green). For each condition, the xy-image shows the overlap of red (hydrogel) and green (fibronectin) channels. Dotted lines on the xy-images represent the position of the corresponding xz-scans. Scale bars are 50 μm.

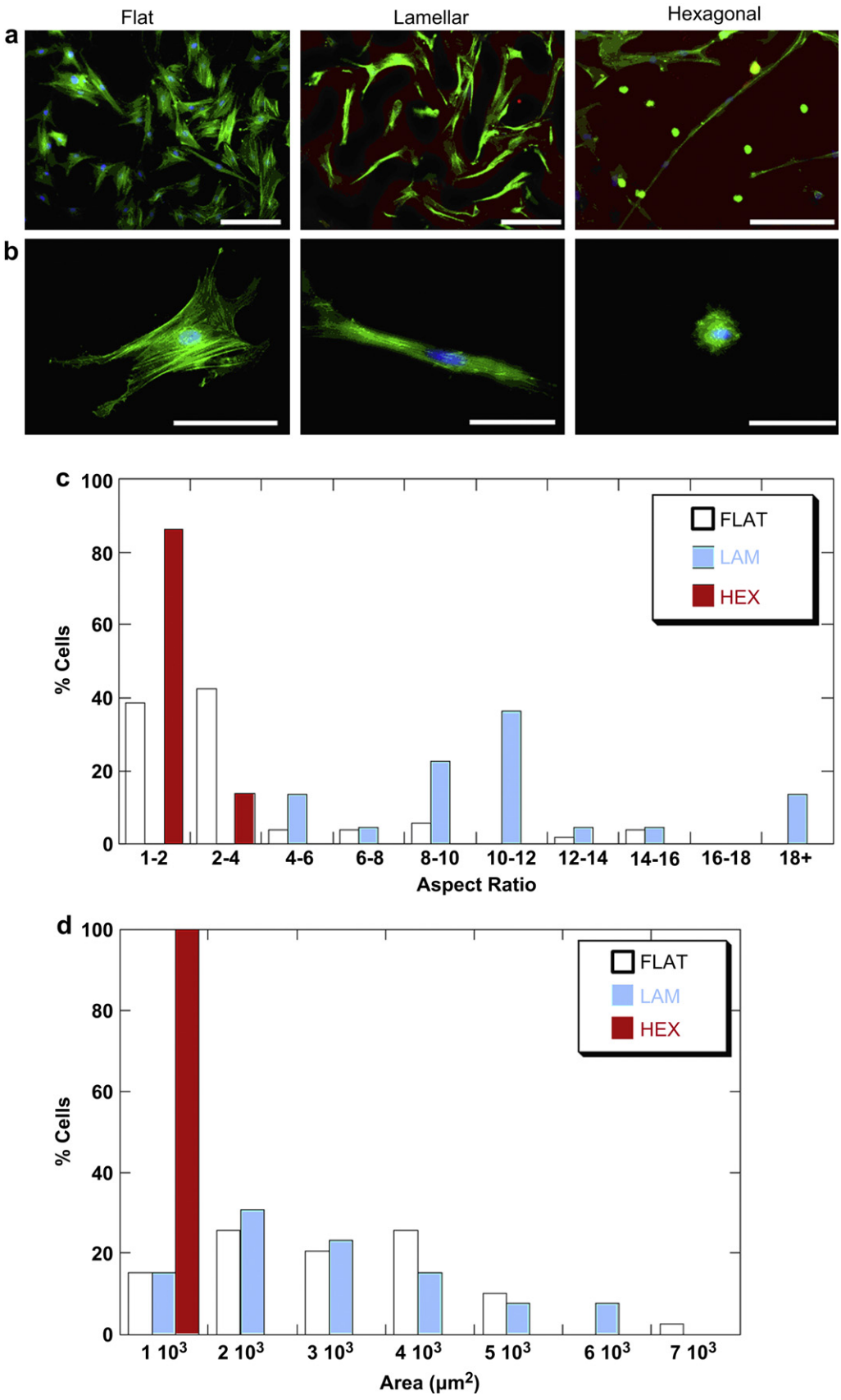

Fig. 3. Fluorescent microscopy images of hMSCs seeded on flat (FLAT), lamellar (LAM) and hexagonal (HEX) hydrogel patterns (staining: blue-nuclei, green-actin, and red-hydrogel) and cultured for 24 h (a–b) Images showing typical stem cell morphology and spreading: random for flat, spread and elongated for lamellar, and rounded with small area for hexagonal patterns. Stem cell aspect ratio (c) and spreading (d) for flat, lamellar and hexagonal hydrogels. Scale bars are 100 μm for top panel and 25 μm for bottom panel.

hydrogel independent of the surface topography (Fig. 2). Thus, the concentration of fibronectin is uniform on all surfaces at the cell-material interface.

HMSCs were seeded on fibronectin-adsorbed PHEMA replica hydrogels with lamellar and hexagonal surface patterns and allowed to attach and spread for 24 h. The cells were then fixed and co-stained for actin (green) and nuclei (blue) to determine the shape (aspect ratio, AR), spreading (cell area) and number of hMSCs (Fig. 3a and b). A fluorescent marker was incorporated into the precursor solution prior to UV exposure to obtain contrast from the hydrogel under fluorescence (red). HMSCs were found to attach and spread randomly onto the flat hydrogels, such that almost 80% of the cells had an AR between 1 and 4, whereas the remaining 20% had AR between 4 and 16 (Fig. 3). In addition, the cell area varied randomly from 1×10^3 to 7×10^3 μm^2. On wrinkled hydrogel surfaces, the ability of hMSCs to recognize the pattern geometry was found to be dependent on the pattern size, and the stem cell morphology was determined by the location of the cell relative to the pattern (i.e., inside the pattern grooves or on the pattern surface, see Fig. S1 in the Supporting Information). This, we believe, is due to the relatively large length scale of the patterns compared to the stem cells.

For lamellar patterns with $\lambda \sim 50$ μm, the majority of the cells (~90%) were located on the pattern surface, spread randomly without recognizing the pattern, and mostly formed bridges between the patterns (Fig. S1 in the Supporting Information). However, for $\lambda \sim 100$ μm, the majority of cells (~80%) aligned themselves along the patterns (Fig. 3a and c) with a wide distribution of AR from 4 to 30 such that majority of these cells (~40%) had AR within 10–12 followed by 8–10 (23%), 4–6 (14%), and AR > 18 (14%). These cells exhibited a wide range of spreading of $2–6 \times 10^3$ μm^2 (Fig. 3d). For hexagonal patterns with $\lambda \sim 50$ μm, ~36% of the cells attached inside the patterns. These cells were constrained by the groove and remained rounded with AR of 1–2 (88%) and 2–4 (12%) and had uniform cell areas (~1×10^3 μm^2) (Fig. 3c and d). The remaining cell population was found to attach on the patterns (outside grooves) with low AR, but with a wide range of cell areas ($1–4 \times 10^3$ μm^2). When the pattern size was increased to $\lambda \sim 100$ μm, the majority of the cells were found to be inside the patterns with low aspect ratio (AR = 1–2), but large spreading (cell area = $2–7 \times 10^3$ μm^2) (Fig. S1 in the Supporting Information). The cells that were outside the patterns were well spread ($1–5 \times 10^3$ μm^2) with AR mostly in the range of 1–6. These results show that the morphology and size of the hydrogel surface wrinkle controls the attached stem cell shape and spreading.

It has been shown that cell spreading (elongated or cuboidal) facilitates calcium deposition during bone remodeling in osteocytes [29,30], whereas round cells (circular with low spreading) allows for maximum lipid storage in adipocytes [31,32]. Here, we examined whether the control of cell shape using hydrogel surface wrinkling could direct the hMSC differentiation. To do so, we chose lamellar patterns with $\lambda \sim 100$ μm, where we observed aligned cells with high aspect ratio to stimulate osteogenesis, and hexagonal patterns with $\lambda \sim 50$ μm, where we observed round cells with small area to stimulate adipogenesis (Fig. 3a and b). HMSCs were allowed to attached and spread for 1 day in growth media, followed by 14 days of incubation in 1:1 adipogenic/osteogenic mixed media. The

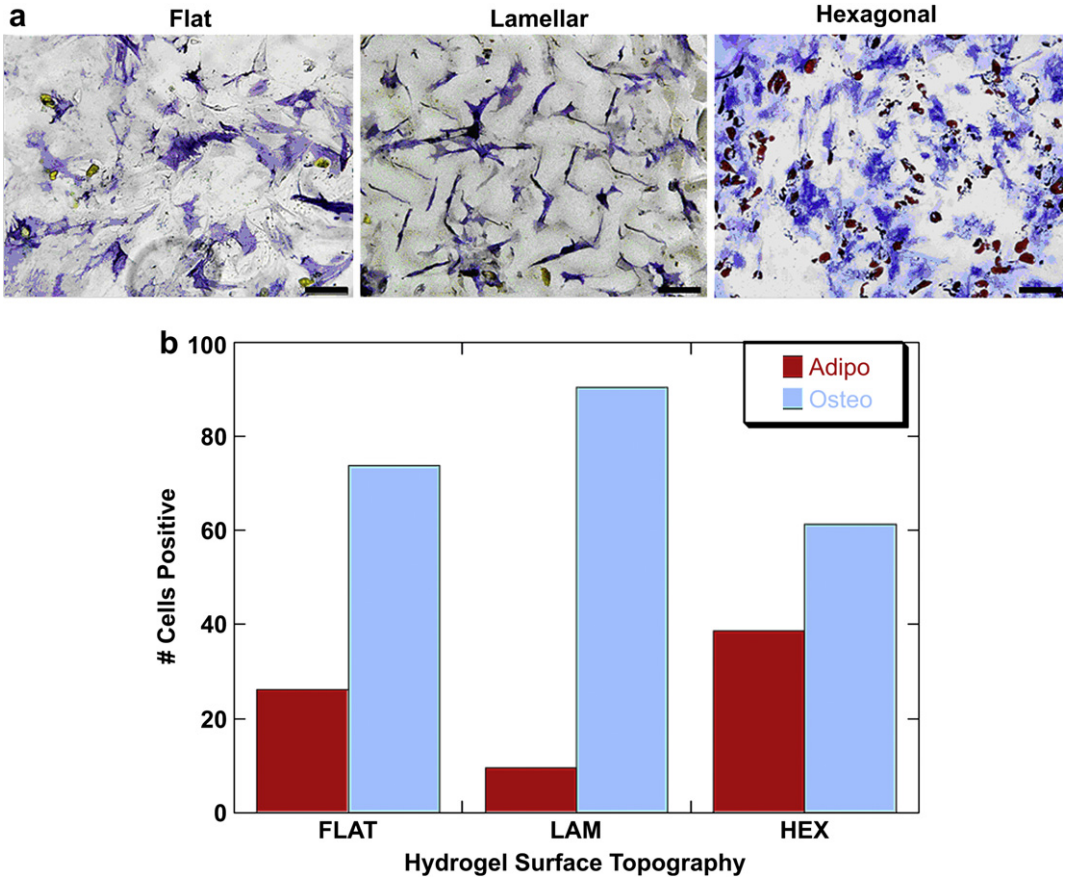

Fig. 4. (a) Optical microscopy images of hMSCs seeded on flat (FLAT) hydrogels and hydrogels with lamellar (LAM) and hexagonal (HEX) patterns and cultured for 14 days in mixed media. Cells are stained for alkaline phosphatase (blue) and oil droplets (red) as markers of osteogenesis and adipogenesis, respectively. Scale bars are 100 μm. (b) Quantification of % cells that were stained positive for either oil droplets (adipo) or alkaline phosphatase (osteo).

cells were then co-stained for alkaline phosphatase as a marker of osteogenesis and oil droplets as a marker of adipogenesis (Fig. 4a). When all cells were quantified, osteogenic differentiation was found to be up-regulated (Fig. 4b) such that ~91% of the cells stained for alkaline phosphatase for lamellar patterns, followed by ~74% for flat gels, and ~61% for hexagonal patterns. Likewise, adipogenic differentiation was found to be up-regulated such that ~39% of the cells stained positive for oil droplets for hexagonal patterns, followed by ~26% for flat gels, and ~9% for lamellar patterns. Cells exhibited minimal differentiation when they were

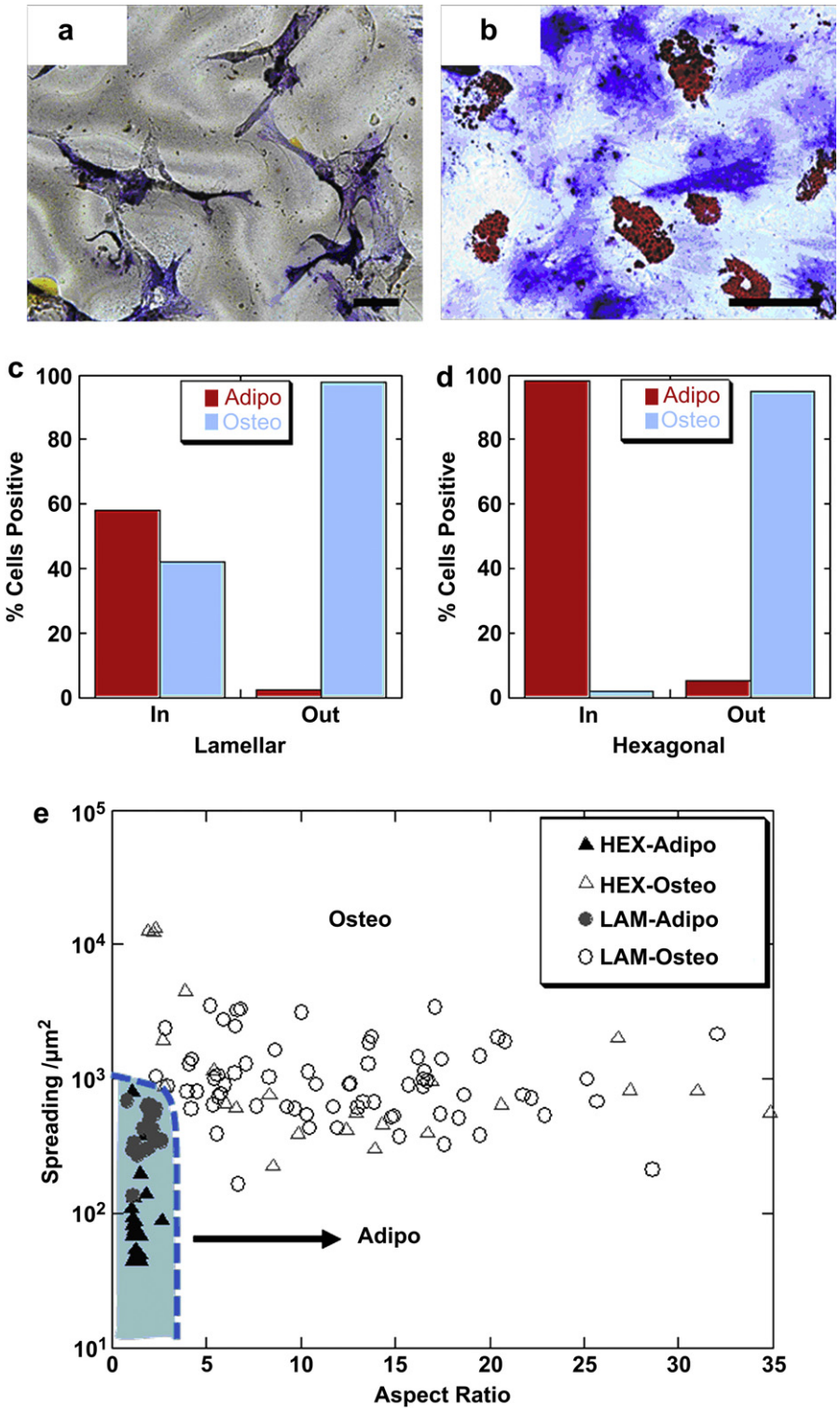

Fig. 5. Optical microscopy images of hMSCs seeded on flat hydrogels and hydrogels with (a) lamellar and (b) hexagonal patterns and cultured for 14 days in mixed media. Cells were stained for alkaline phosphatase (blue) and oil droplets (red) to indicate osteogenesis and adipogenesis, respectively. Scale bars are 50 μm. (c–d) Staining results showing % cells that were stained positive for oil droplets (adipo) and alkaline phosphatase (osteo) for lamellar and hexagonal patterns. Cells that were in the pattern grooves are denoted by "In" and on the patterns by "Out". (e) Spreading versus aspect ratio for overall cell population on lamellar and hexagonal patterns.

incubated in growth media (see Fig. S2 in the Supporting Information).

As described above, the location of an individual cell relative to the pattern determines its shape and spreading (Fig. 3b–c). Therefore, we examined the cells in two groups: "in" and "out", indicating cells adhered inside and outside the grooves, respectively. For lamellar patterns, osteogenic differentiation was up-regulated (~98% of the cells) for cells that were outside the patterns and exhibited high spreading and AR (Fig. 3c–d), in contrast to only a 20% difference in favor of osteogenic differentiation for cells inside the patterns (Fig. 5a and c). For hexagonal patterns, almost all of the cells (~98%) inside the grooves remained rounded with low AR (Fig. 3c–d) and differentiated towards an adipogenic phenotype, whereas the majority of the cells (~95%) that were outside the patterns differentiated towards an osteogenic phenotype (Fig. 5b and d). To further understand this behavior, the cell spread area versus the AR was plotted for both lamellar and hexagonal patterns (Fig. 5e). Regardless of the pattern morphology, we observed that adipogenic differentiation occurred for cells within a certain morphological region, namely spread areas $<10^3$ μm^2 and AR < 4 (see the shaded area in Fig. 5e). Cells outside this region all differentiated into an osteogenic phenotype when cultured in this mixed media formulation. Therefore, these results show that cell spread area becomes very important for determining differentiation for cells with low aspect ratio (AR < 4); within this regime, cells with spread areas $<10^3$ μm^2 and $\geq 10^3$ differentiated down adipogenic and osteogenic lineages, respectively. However, for cells with AR ≥ 4, cells exhibited exclusively an osteogenic phenotype.

To further confirm these findings, cells were stained for other markers of differentiation: i.e., FABP4 and osteocalcin, for adipogenesis and osteogenesis, respectively (see Fig. S3 in the Supporting Information). After 14 days in mixed media, only cells that were elongated and aligned by taking the shape of the lamellar pattern stained positive for osteogenesis (i.e., osteocalcin). In contrast, only cells inside the hexagonal patterns remained round with low spread area and stained positive for FABP4. These results confirmed the selective differentiation of hMSCs on patterned PHEMA hydrogels.

4. Conclusions

In summary, we used hydrogel surface wrinkles to control hMSC morphology and differentiation. We found that cells attached on the lamellar pattern spread by taking the shape of the pattern, exhibited high AR, and differentiated into an osteogenic phenotype. In contrast, cells that attached inside the hexagonal patterns remained rounded with low spreading and differentiated into an adipogenic phenotype. Collectively, our results clearly indicate the influence of cell morphology and spreading on differentiation, particularly when investigated in relatively soft hydrogel systems, as compared to previous work on flat rigid surfaces. These results are important in that they can help define culture conditions that permit selective differentiation, may provide information on material surfaces for implantation, and may define scaffold structures that dictate desired lineage specification, including with spatial control based on surface morphology.

Acknowledgements

The authors would like to acknowledge funding from a David and Lucile Packard Foundation Fellowship in Science and Engineering and a National Science Foundation CAREER Award. The authors are also grateful to Sudhir Khetan, Ross Marklein, and Yang-Kao Wang for helpful discussions and protocols and to Gladys Grey-Board for assistance with confocal microscopy. (Supporting Information is available online from Wiley InterScience or from the author).

Appendix. Supplementary data

Supplementary data associated with this article can be found in the online version, at doi:10.1016/j.biomaterials.2010.05.037.

Appendix

Figures with essential colour discrimination. Figs. 2 and 3 of this article may be difficult to interpret in black and white. The full colour images can be found in the online version at doi:10.1016/j.biomaterials.2010.05.037.

References

[1] Caplan AI. Mesenchymal stem-cells. J Orthop Res 1991;9(5):641–50.
[2] Pittenger MF, Mackay AM, Beck SC, Jaiswal RK, Douglas R, Mosca JD, et al. Multilineage potential of adult human mesenchymal stem cells. Science 1999;284(5411):143–7.
[3] Sasaki M, Abe R, Fujita Y, Ando S, Inokuma D, Shimizu H. Mesenchymal stem cells are recruited into wounded skin and contribute to wound repair by transdifferentiation into multiple skin cell type. J Immunol 2008;180(4):2581–7.
[4] Stappenbeck TS, Miyoshi H. The role of stromal stem cells in tissue regeneration and wound repair. Science 2009;324(5935):1666–9.
[5] Allen LT, Fox EJP, Blute I, Kelly ZD, Rochev Y, Keenan AK, et al. Interaction of soft condensed materials with living cells: phenotype/transcriptome correlations for the hydrophobic effect. Proc Natl Acad Sci U S A 2003;100(11):6331–6.
[6] Brodbeck WG, Shive MS, Colton E, Nakayama Y, Matsuda T, Anderson JM. Influence of biomaterial surface chemistry on the apoptosis of adherent cells. J Biomed Mater Res 2001;55(4):661–8.
[7] Garcia AJ, Vega MD, Boettiger D. Modulation of cell proliferation and differentiation through substrate-dependent changes in fibronectin conformation. Mol Biol Cell 1999;10(3):785–98.
[8] Keselowsky BG, Collard DM, Garcia AJ. Integrin binding specificity regulates biomaterial surface chemistry effects on cell differentiation. Proc Natl Acad Sci U S A 2005;102(17):5953–7.
[9] McClary KB, Ugarova T, Grainger DW. Modulating fibroblast adhesion, spreading, and proliferation using self-assembled monolayer films of alkylthiolates on gold. J Biomed Mater Res 2000;50(3):428–39.
[10] Discher DE, Janmey P, Wang YL. Tissue cells feel and respond to the stiffness of their substrate. Science 2005;310(5751):1139–43.
[11] Engler AJ, Sen S, Sweeney HL, Discher DE. Matrix elasticity directs stem cell lineage specification. Cell 2006;126(4):677–89.
[12] Burdick JA, Vunjak-Novakovic G. Engineered microenvironments for controlled stem cell differentiation. Tissue Eng Part A 2009;15(2):205–19.
[13] Discher DE, Mooney DJ, Zandstra PW. Growth factors, matrices, and forces combine and control stem cells. Science 2009;324(5935):1673–7.
[14] Marklein RA, Burdick JA. Controlling stem cell fate with material design. Adv Mater 2010;22(2):175–89.
[15] Carvalho RS, Schaffer JL, Gerstenfeld LC. Osteoblasts induce osteopontin expression in response to attachment on fibronectin: demonstration of a common role for integrin receptors in the signal transduction processes of cell attachment and mechanical stimulation. J Cell Biochem 1998;70(3):376–90.
[16] Spiegelman BM, Ginty CA. Fibronectin modulation of cell-shape and lipogenic gene expression in 3T3-adipocytes. Cell 1983;35(3):657–66.
[17] Thomas CH, Collier JH, Sfeir CS, Healy KE. Engineering gene expression and protein synthesis by modulation of nuclear shape. Proc Natl Acad Sci U S A 2002;99(4):1972–7.
[18] McBeath R, Pirone DM, Nelson CM, Bhadriraju K, Chen CS. Cell shape, cytoskeletal tension, and RhoA regulate stem cell lineage commitment. Dev Cell 2004;6(4):483–95.
[19] Ruiz SA, Chen CS. Emergence of patterned stem cell differentiation within multicellular structures. Stem Cells 2008;26(11):2921–7.
[20] Kilian KA, Bugarija B, Lahn BT, Mrksich M. Geometric cues for directing the differentiation of mesenchymal stem cells. Proc Natl Acad Sci U S A 2010;107(11):4872–7.
[21] Flemming RG, Murphy CJ, Abrams GA, Goodman SL, Nealey PF. Effects of synthetic micro- and nano-structured surfaces on cell behavior. Biomaterials 1999;20(6):573–88.
[22] Oh S, Brammer KS, Li YSJ, Teng D, Engler AJ, Chien S, et al. Stem cell fate dictated solely by altered nanotube dimension. Proc Natl Acad Sci U S A 2009;106(7):2130–5.
[23] Teixeira AI, Abrams GA, Bertics PJ, Murphy CJ, Nealey PF. Epithelial contact guidance on well-defined micro- and nanostructured substrates. J Cell Sci 2003;116(10):1881–92.

[24] Uttayarat P, Toworfe GK, Dietrich F, Lelkes PI, Composto RJ. Topographic guidance of endothelial cells on silicone surfaces with micro- to nanogrooves: orientation of actin filaments and focal adhesions. J Biomed Mater Res A 2005;75A(3):668–80.
[25] Guvendiren M, Yang S, Burdick JA. Swelling-induced surface patterns in hydrogels with gradient crosslinking density. Adv Funct Mater 2009;19 (19):3038–45.
[26] Guvendiren M, Burdick JA, Yang S. Kinetic study of swelling-induced surface pattern formation and ordering in hydrogel films with depth-wise cross-linking gradient. Soft Matter 2010;6(9):2044–9.
[27] Chung C, Burdick JA. Influence of three-dimensional hyaluronic acid micro-environments on mesenchymal stem cell chondrogenesis. Tissue Eng Part A 2009;15(2):243–54.
[28] Khetan S, Katz JS, Burdick JA. Sequential crosslinking to control cellular spreading in 3-dimensional hydrogels. Soft Matter 2009;5(8):1601–6.
[29] Parfitt AM. Age-related structural-changes in trabecular and cortical bone – Cellular mechanisms and biomechanical consequences. Calcif Tissue Int 1984;36:S123–8.
[30] Sikavitsas VI, Temenoff JS, Mikos AG. Biomaterials and bone mechano-transduction. Biomaterials 2001;22(19):2581–93.
[31] Gregoire FM, Smas CM, Sul HS. Understanding adipocyte differentiation. Physiol Rev 1998;78(3):783–809.
[32] Grigoriadis AE, Heersche JNM, Aubin JE. Differentiation of muscle, fat, cartilage, and bone from progenitor cells present in a bone-derived clonal cell-population – effect of dexamethasone. J Cell Biol 1988;106(6): 2139–51.